

29 1. Introduction

30 Gold is a rare and precious metal that is widely used in various manufacturing industries such as
31 smart phones, personal computers (PCs), and other electrical printed circuit boards (PCBs) based
32 electronic devices due to its excellent physical & chemical properties, electrical properties, high
33 catalytic activity and strong coordination ability[1-3]. However, the huge amounts of electronic scraps
34 are also generated because of the technological innovations and a subsequent short lifetime of
35 electronic devices [4-5]. PCBs are the key components and are considered as the most valuable parts
36 among electric and electronics equipments, since they contain precious metals in higher concentrations
37 than natural high-grade ores. For example, PCBs used in smart phones and PCs contain gold of about
38 280g /ton-waste, which is very high compared to 3-5 g/ton of gold in naturally occurring gold ores[5-6].
39 In addition, natural occurrences of these precious metals are limited and, in some mines, already
40 depleted. Hence, to meet the increasing demand for gold, separation and recovery of gold from PCBs
41 must be undertaken. The recovery of precious metals like gold from secondary sources is quite
42 important from economic and environmental points of view [4, 7] .

43 Conventional methods such as precipitation, ion exchange, solvent extraction, and flotation for gold
44 recovery are available, but these methods have major disadvantages like the use of toxic chemicals,
45 high reagent requirements and generation of toxic secondary waste that required disposal[8-11].
46 Various biomasses have been used as biosorbent for recovery of precious metals, but they have major
47 limitations in terms of low adsorption capacity, selectivity and reusability [12-15].

48 Bio-mineralization is natural phenomena and the process by which living organisms produce
49 minerals. Bacterial mineralization is generally selective for elements[16-18]. For example,
50 magnetotactic bacteria form magnetosomes in vivo by selectively absorbing iron in solution [19-20].
51 Bacterial mineralization to recovery metals has been gained a lot of attentions because of moderate
52 reaction conditions, without toxic chemicals and good metal selectivity [21-23]. It reported that
53 *Cupriavidus metallidurans* were responsible for the formation of secondary gold nano-mineral in the
54 periplasmic space, which indicated that the production of secondary gold nano-mineral may be
55 concerned with cell active reduction[24]. However, *Delftia acidovorans* induce gold ions
56 mineralization by secreted delftibactin(a small molecule peptide) in solution[17]. Apart from the
57 biological accumulation of AuNPs in prokaryotes, eukaryotes have also been reported to form gold
58 nano-particles by biomineralization [23, 25-26].

59 This paper focuses on the development of low-cost and eco-friendly method for recovery of gold
60 from multi-ionic aqueous systems via bacterial mineralization[12]. The *Bacillus licheniformis* FZUL-
61 63, separated from a landscape lake in FuZhou University, was shown to selectively mineralize and
62 precipitate gold from coexisting ions in aqueous solution. The process is as follows: Au(III) ions are
63 reduced to monovalent by the *B. licheniformis*, and then the Au(I) was adsorbed on the bacterial surface
64 at the beginning stage(first hour). The amino, carboxyl and phosphate groups on the surface of the
65 bacteria are related to the adsorption of gold ions. The gold biomineralization began about 10 hours
66 after the interaction between Au(III) ions and bacteria and has been rarely influenced by other co-
67 existing metal ions. The formed gold nanoparticles are polyhedral structure with a particle size of ~20
68 nm. The bacteria could selectively mineralize and recover 478 mg/g(dry biomass) gold from aqua
69 regia-based metal wastewater through 4 cycles. It could be of great potential in recovering Au(III) from
70 multi-ionic aqueous systems.

71 2. Materials and methods

72 2.1. Microorganisms and growth conditions

73 The strain FZUL-63, isolated from a landscape lake in FuZhou University, China (GPS location: N
74 22°03.41 E 119°11.23), was identified through 16S rDNA sequence homology analysis based on the
75 standard procedure[27]. The strain FZUL-63 was cultivated in LB medium with 1% Tryptone, 0.5%
76 Yeast and 1%NaCl for 2d at 30°C. The cells were collected via centrifugation at 9,000 rpm for 10 min
77 and the sediment was washed with 0.9% NaCl for three times, and then the cells was re-suspended in
78 the 0.9% NaCl for the variation analysis. In order to prevent the formation of silver chloride
79 precipitation, we use purified water instead of 0.9% NaCl to wash and re-suspend the cells that are
80 acting with silver.

81 2.2. Metals ion solution and analysis

82 All the chemicals used in this work were of analytical grade and were obtained from Sigma-
83 Aldrich or Aladdin Industrial Corporation. Reagent grade water with a specific resistance of 18.2 M cm
84 was obtained from a Milli-Q water purification system. The stock solution (1,000mg/L) of Au(III),
85 Cu(II), Pt(III), Cr(VI), Pb(II), Ag(I), Zn(II) used in this experiments were prepared by dissolving
86 $\text{HAuCl}_4 \cdot 3\text{H}_2\text{O}$, $\text{CuSO}_4 \cdot 5\text{H}_2\text{O}$, HPtCl_4 , $\text{K}_2\text{Cr}_2\text{O}_7$, PbNO_3 , AgNO_3 and $\text{ZnSO}_4 \cdot 7\text{H}_2\text{O}$ with purified water,
87 respectively. The standard solution ranging from 1 to 200 mg/L of the metals ion were prepared by
88 diluting the stock solutions. Adjustment of pH was carried out using 0.1 mol/L NaOH or 0.1 mol/L
89 HNO_3 . The concentration of the metals ion was measured by ICP-OES (Optima 7000 DV, PerkinElmer,
90 USA).

91 2.3. Au(III) uptake and mineralization experiments

92 The harvested and washed bacterial cells were transferred into a 100-mL triangular flask containing
93 30 mL Au(III) solution (200 mmol/L). The bacterial concentration was 0.05 mg/mL (dry weight) and
94 pH was maintained at 7 in the initial point of the experiment. No nutrients were added to the reactors.
95 Subsequently, the triangular flask was incubated at 30 °C with a constant shaking speed of 160 rpm.
96 Subsamples were collected at predetermined times and centrifuged at 5400g for 10 min. The
97 supernatant samples were filtered through 0.22- μm filters to remove Au(III) adsorbed on cell fragments.
98 The residual Au(III) concentration in aqueous solution was determined by ICP-OES. All experiments

99 were performed in triplicate.

100 The precipitates were freeze-dried and ground to powder in a mortar. The powder samples were
101 analyzed by XRD (MiniFlex600, Rigaku, Japan) with $\text{CuK}\alpha$ ($\lambda = 0.154$ nm), incident beam
102 monochromator, and power of $40 \text{ kV} \times 20 \text{ mA}$ [28]. Diffractograms were obtained over a 2θ range of 5
103 to 80° at a speed of $2^\circ/\text{min}$. Peak identification was achieved with a standard profile fitting routine
104 provided by Philips Netherlands. Qualitative identification of mineral phases was made utilizing the
105 MDI Jade 7 software[29]. The average size of the metal gold particles was calculated by Sherrer
106 procedure.

107 TEM/EDS were employed to observe the distributions of Gold on the bacteria cells. After complete
108 interaction of Au(III) (24 h of incubation), a 2-mL cell-Au(II) suspension was taken from the 200mg/L
109 Au(III) bio-removal experiment and centrifuged at 5400g for 10 min. The resulting cell pellet was
110 washed three times with DI water. JEOL JEM-2100 LaB6 TEM with an accelerating voltage of 200
111 keV fitted with STEM/EDS was employed for high resolution imaging and for compositional analysis.
112 To identify the reduced gold mineral, selected area electron diffraction (SAED) pattern was acquired
113 with a Gatan Orius SC200D camera[30].

114 Scanning electron microscopy (SEM) and elemental mapping were employed to observe the
115 distributions of Gold on the bacteria cells. SEM observations were made to identify any morphological
116 changes of *B. licheniformis* upon exposure of Gold(III) and to identify any mineral phase formed from
117 Au(III) adsorption. Among the four different Au (III) concentrations used for the adsorption experiment,
118 the 3.75 mM Au(III) sample was observed under SEM. Cells were first fixed for 20 min with 2%
119 formaldehyde and 2.5% glutaraldehyde in a 0.05-M sodium cacodylate buffer (pH 7.2) at a 1:1 ratio
120 (sample: fixative). After this primary fixation, a few drops of sample suspension were placed over the
121 surface of a glass cover slip and sequentially dehydrated using varying proportions of ethanol followed
122 by critical point drying with a Tousimis Samdri-780A critical point dryer (CPD). Critical point dried
123 samples were coated with carbon using Denton vacuum evaporator DV-502A. A Zeiss Supra 35 VP
124 SEM with Genesis 2000 Xray energy-dispersive spectroscopy (SEM/EDS) was employed for cell
125 imaging and compositional analyses (Bishop et al. 2014).

126 **2.4 X-ray photoelectron spectroscopy (XPS) analysis**

127 The chemical states of gold in the samples were measured by XPS. The powder samples of
128 bacteria reacting with Au(III) for different time were placed in an evacuated sample chamber.
129 Survey spectra were collected over the range of 0~1200 eV with pass energy of 30.0 eV. High-
130 resolution XPS spectra were acquired for C1s[31]. All binding energy values were calibrated by
131 using the value of contaminant carbon (284.65 eV) as a reference[32]. The spectra for Au were
132 obtained under conditions of 0.05 eV step and analyzed after corrections.

133 **2.5 Selective Mineralization experiments**

134 The common metal ions in electroplating wastewater include Au(III), Cu(II), Pt(III), Cr(VI), Pb(II),
135 Ag(I), Zn(II) and so on. The above mentioned ions are prepared at every 100-mL triangular flask by
136 diluting the stock solution, respectively. The gold stock solution is added to the various triangular flasks
137 with the initial concentration 200mg/L except triangular flask contain the Ag(I) solution (Because Ag(I)
138 ions cannot coexist with the $\text{HAuCl}_4 \cdot 3\text{H}_2\text{O}$ solution). After adding the Au(III), the initial
139 concentration of Cu(II), Pt(III), Cr(VI), Pb(II), Ag(I), Zn(II), were adjusted to 200mg/L and the
140 bacterial dosage was 5g dry weight per liter in each 100-mL triangular flask containing 25 mL solution.
141 Subsequently, the triangular flasks were incubated at 30 °C with a constant shaking speed of 160 rpm.
142 Subsamples were collected at predetermined times and centrifuged at 5400g for 10 min. The residual
143 ions concentrations in the supernatant were determined by ICP-OES and the pellet were analysis by
144 XRD and TEM as mentioned above.

145 **2.6 Recovery of Au(III) form aqua regia-based metal wastewater**

146 Remove as much other metal as possible except for gold ions from the circuit printing plate with
147 nitric acid. The insoluble substance was collected and treated with aqua regia. And then adjust pH to
148 6.0 with 5 mol/L KOH and centrifuge. The metal ion concentrations in the supernatant, also call it aqua
149 regia-based metal wastewater were determined by ICP-OES as mentioned above.

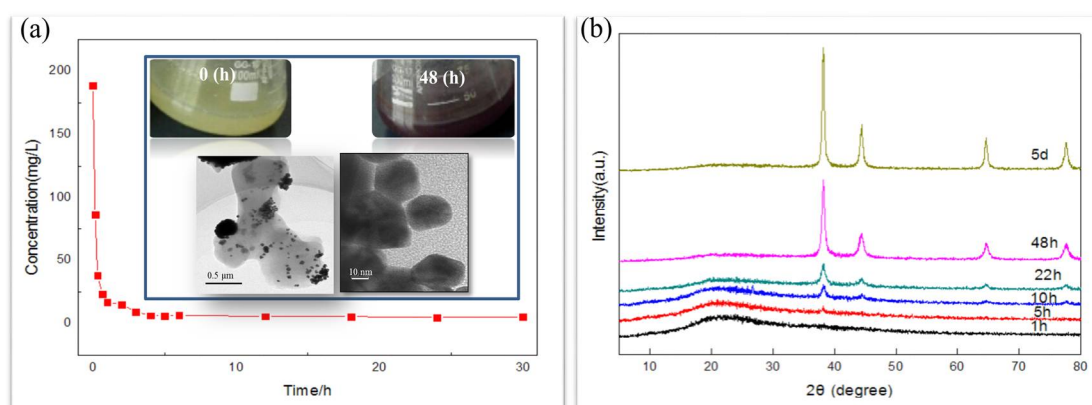
150 The bacteria were added to the supernatant with the amount of 1 grams biomass(dry weight) per liter.
151 Subsequently, the triangular flasks were incubated at 30 °C with a constant shaking speed of 160 rpm.
152 Subsamples were collected at predetermined times for analysis. Reach the reaction platform stage,
153 bacteria and gold nanoparticles were collected by centrifugation at 5400g for 10 min, and the aqua

154 regia-based metal wastewater was added to the collection contained bacteria and gold nanoparticles
155 again. Cycle many times until the bacteria have less or no ability to mineralize Au(III).

156 3. Results and discussion

157 3.1 Au(III) uptake and mineralization

158 The strain FZUL-63 was identified as *Bacillus licheniformis* through 16S rDNA sequence homology
159 analysis. *B. licheniformis* removed Au(III) from aqueous solution as a function of time. The Au(III)
160 concentration in aqueous solution showed a time-course decrease, from 200 to 4.975 mg/L, and after
161 one hour of interaction Au (III) concentration reached a steady state (Fig. 1a). In this process, the color
162 of the culture in the triangular flask turns from bright yellow to pink (10 hours), and finally becomes
163 wine red (Fig. 1a). The solid phase samplings collected from different interaction time were analyzed
164 by XRD (Fig. 1b). In first hour, no peaks were detected on XRD patterns after the interaction between
165 bacteria and Au(III), suggesting that adsorbed Au (III) did not form a crystalline phases. Although no
166 crystalline phases were detected with XRD after one hour interaction, with prolonged time, some weak
167 peaks were observed on XRD pattern after 10 hours of interaction, implying that a small amount of
168 gold mineral formed (Fig. 1b). The newly observed diffraction peaks matched well with gold
169 nanoparticles [Au(PNs)]. These results suggest that with time the bacterium may have mediated Au (III)
170 transformation from amorphous compound to a stable AuNPs. Under TEM, there were many AuNPs
171 with a ~20 nm grain size on and around bacterial cell surface (Fig. 1a).



172
173 Fig 1. The interaction between bacteria and Au(III) with time. (a). The Au(III) concentration in aqueous
174 solution showed a time-course decrease. (b). XRD pattern of the Au(PNs) enhanced over time.

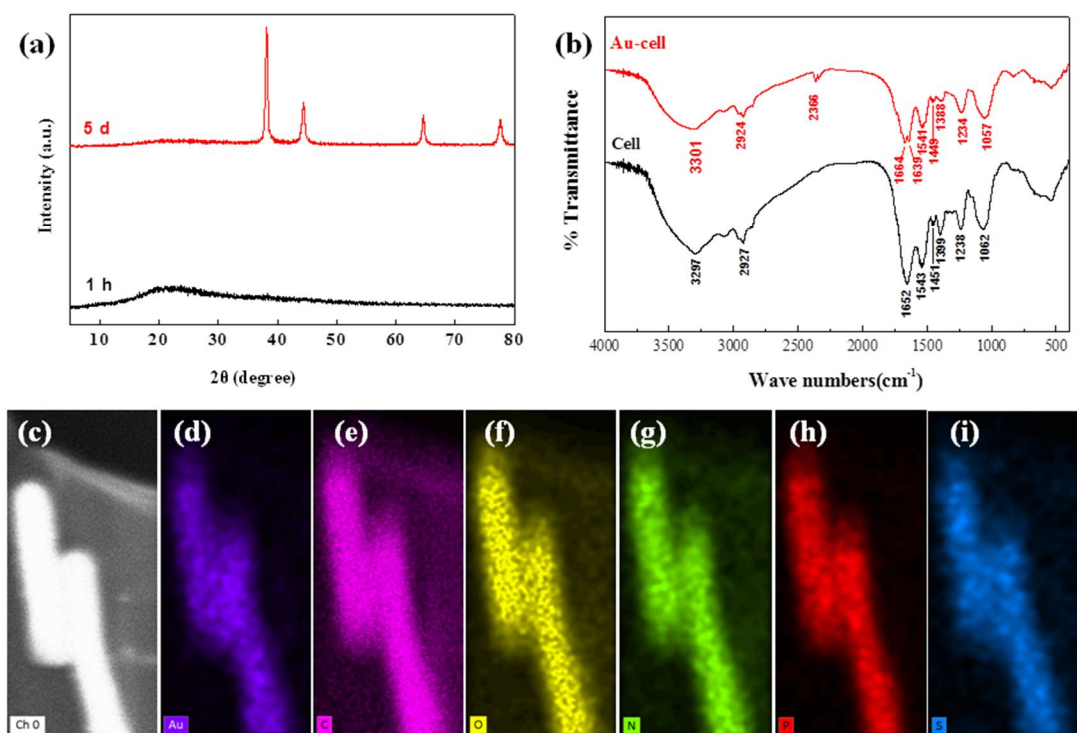
175

176 3.2 The chemical groups involved in gold binding

177 The gold ions in the aqueous solution is quickly removed (Fig. 1a), but the XRD results indicate
178 that no minerals have been formed at the initial stage (Fig. 1b), so the gold ions may be adsorbed on the
179 surface of the bacteria first. To elucidate the chemical groups involved in gold binding, FTIR spectra
180 were recorded for control and gold loaded cells from 4000 cm^{-1} to 400 cm^{-1} (Fig. 2).

181 The characteristic peaks can be assigned to the involvement of the main functional groups present
182 in the bacterial biomass by analyzing the highly complex IR spectra (Fig. 2). The N–H stretching peak
183 lies in the spectrum region occupied by a broad and strong band in 3200–3600 cm^{-1} region was due to
184 the presence of γ O–H of the hydroxyl groups, which undergo change in peak position in gold loaded
185 spectrum suggesting the involvement of amino and hydroxyl groups in gold binding to bacterial
186 surface[33-34]. In the spectra for gold loaded cell the peak around 2366 cm^{-1} could be assigned to the
187 P–O stretching vibrations implying possible role of phosphate metabolism facilitating cellular
188 adsorption of gold ions. The spectra for both control and gold loaded samples revealed protein related
189 bands. The appearance of γ C=O of amide I and δ NH/ γ C=O combination of the amide II bonds at
190 were present at 1652 cm^{-1} and 1543 cm^{-1} , respectively were predominant in the control spectrum.
191 Following Au binding, the amide I absorption peak (1652 cm^{-1}) was split in to two minor peaks at 1664
192 cm^{-1} and 1639 cm^{-1} and a marked shift of 1543 cm^{-1} peak to 1541 cm^{-1} suggest a strong interaction of
193 Au with carboxyl groups. In the control spectrum, sharp peaks in between 1400 cm^{-1} and 1500 cm^{-1}
194 were due to the presence of the carboxyl groups [31]. Particularly, the strong peak at 1451 cm^{-1} which
195 was characteristic of the scissoring motion of CH₂ groups [32] undergo a shift to lower energy level
196 (1449 cm^{-1}) after gold binding. Following gold uptake a clear shift of the peak at 1399 cm^{-1} to 1388
197 cm^{-1} due to symmetric stretching of COO⁻ vibration strongly indicated role of carboxyl groups in gold
198 binding[34]. In the control spectrum, the strong peaks at 1238 cm^{-1} and 1062 cm^{-1} were observed due
199 to vibrations of carboxyl and phosphate groups[35]. Following gold exposure, a clear shift of these
200 peaks to 1234 cm^{-1} and 1057 cm^{-1} suggests interaction of bound metals with carboxyl and phosphates
201 groups. A gradual shift of the peak in control spectra at 1239 cm^{-1} because of asymmetric stretching
202 modes of protonated polyphosphates and PO uncomplexed in phosphate diesters to 1238 cm^{-1} in gold
203 loaded samples indicated the weakening of the P=O character as a result of metal binding to the
204 phosphates[35]. Changes in peak position and intensity at 800 cm^{-1} to 400 cm^{-1} region could be
205 assigned to the formation of intense (M–O) and (O–M–O) bonds (M =metal ion)[33]. The overall IR
206 spectroscopic analysis suggests that phosphate, carboxyl and amide groups on bacterial cell are the

207 dominant functional groups involved in bacteria-gold interaction.



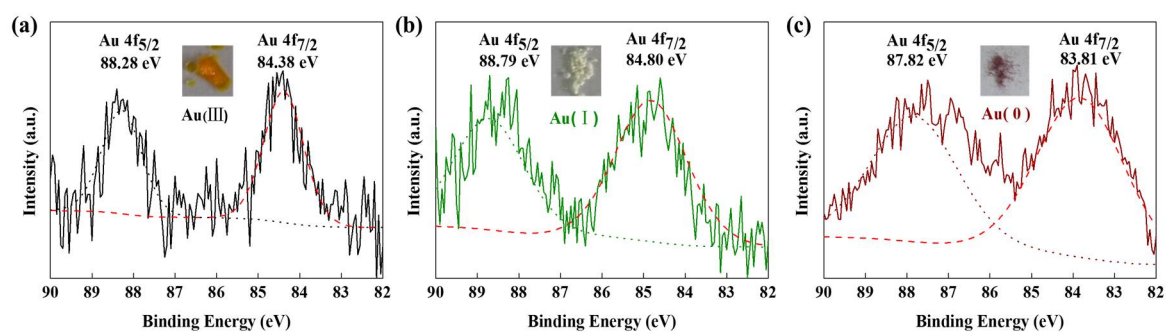
208

209 Fig. 2. Fourier transformed Infra Red spectra of *B. licheniformis* FZUL-63 biomass: before and after
 210 gold uptake (initial concentration 200 mg Au (III) L⁻¹ at pH 6.0, time 1 h).
 211

212 3.3 Changes in the chemical valence state of Gold

213 The interaction of Au(III) with bacteria at different time have been investigated by XPS. The Au
 214 4f spectra of all the investigated samples are shown in Fig. 3. The evidence is confirmed by the curve-
 215 fitting of the Au 4f core-level spectra by two spin-orbit splitted Au 4f7/2 and Au 4f5/2 components (DE:
 216 ~ 4.0 eV), showing increasing BE values that correspond to a different chemical state of gold particles
 217 in the samples. In the initial addition of chloric acid sample the Au 4f7/2 photoelectronic peak is
 218 located at BE = 84.38 eV and this value is typical of Au(III) species Fig. 3a. After the interaction of the
 219 trivalent gold ions with bacteria, in the one hour sample shown in Fig. 3b and the Au 4f 7/2 spectrum
 220 consists of only one components located at BE = 84.80 eV, which can be assigned to Au(I) species. In
 221 the 48 hours sample the Au 4f7/2 peak detected at BE = 83.81 eV shown in Fig. 3c can be attributed to
 222 the presence of Au(0) species on the bacteria surface. From the changes in the valence state after the
 223 action of trivalent gold ions and bacteria, it could be deduced that trivalent gold ions are not reduced to
 224 zero-valent gold(AuNP) in one step and the intermediates of monovalent gold compounds were

225 produced in the reduced process.



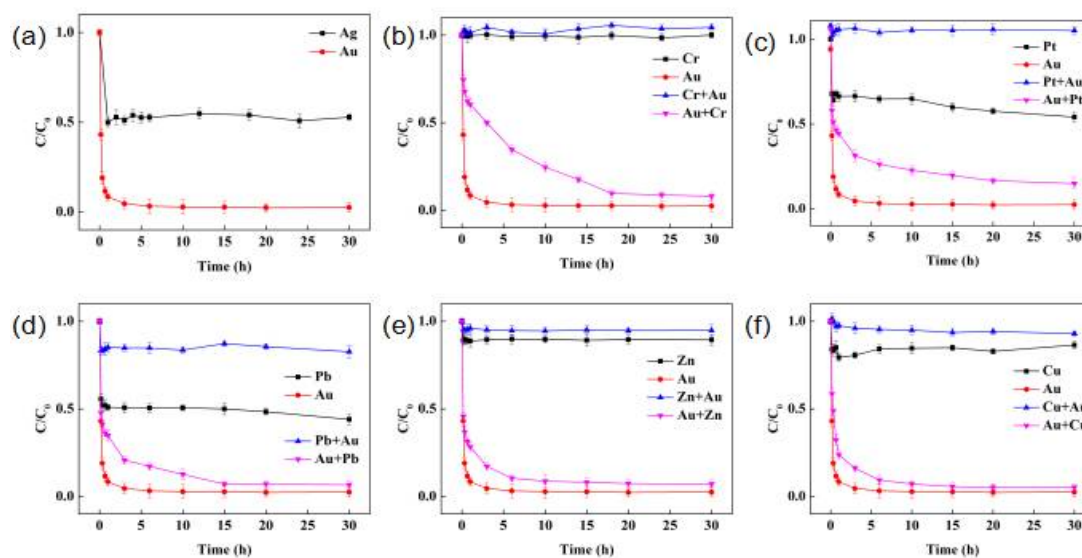
226 Fig. 3 XPS spectra of Au(4f) region of interaction with bacteria for 0 h(a), 1h (b) and 48h(c).

227

228 3.3 Coexisting ions affect the mineralization and recovery of gold

229 The aqua regia-based metal wastewater usually contains the following metal ions such as Au(III),
 230 Pt(III), Ag(I), Cr(VI), Pb(II), Zn(II), Cu(II). The chloroauric acid and the silver ion cannot coexist in
 231 the solution. Therefore, we only did experiments using gold and silver acting alone with bacteria, their
 232 recovery rates were 97.66 and 49.23, respectively (Fig 4 a). The 200 mg/L Cr(VI) ions could delay the
 233 recovery balance time of the gold from 1 hours to 18 hours, the recovery rate of gold was also reduced
 234 from 97.66% to 91.93% (Fig 4 b). Zn(II) and Cu(II) almost rarely influenced the Au(III) recovery
 235 (Fig 4 c, d). However, when the 200 mg/L Pt(III) or Pb(II) coexisting with the Au(III), the recovery
 236 rate of gold was reduced from 97.66% to 85.06% and 93.31%, respectively (Fig e, f).

237 On the contrary, when these ions coexist with the gold ions, the gold ions could competitively
 238 reduce the adsorption of bacteria to these co-existing ions, especially Pt and Pb ions have obvious
 239 reduction. Compared with the removal rate of Pt(III) and Pb(II) via bacteria alone, the removal rate of
 240 Pt(III) and Pb(II) decreased from 45.82% to less 0.5% and 56% to 17.33% in the presence of gold ions,
 241 respectively (Fig 4. c, d). This facilitates the selective recovery of gold from multi-ionic aqueous
 242 systems.



243

244 Fig 4. Au(III) recovery influenced by coexist metal ions. The initial concentration of each ion is

245 200mg/L, and the bacterial dosage is 1g dry weight per liter.

246 **3.4 Recovery of Au(III) form metal wastewater**

247 The CPBs is treated with strong nitric acid. The insoluble substance was collected by
 248 centrifugation and treated with aqua regia. And then adjust pH to 6.0 and centrifuge. The concentration
 249 of ions in the supernatant was measured by ICP, and the concentration of each ion before and after
 250 bacterial treatment was shown in table 1.

251 Table 1 Recovery of Au(III) from aqua regia-based metal wastewater at first cycle.

Metal concn. mg/L	Au ³⁺	Cu ²⁺	Zn ²⁺	Pb ²⁺	Pt ⁴⁺	Cr ⁶⁺	Fe ³⁺	Ni ²⁺	Ag ⁺
Without Cell	181.2±3.2	348.5±3.7	120.0±2.3	39.2±2.6	16.1±1.1	27.3±2.4	85.4±3.5	48.7±2.9	ND
With Cell	17.4±1.2	330.7±2.5	115.2±2.2	34.3±1.7	15.9±1.3	26.1±1.9	80.6±3.1	47.3±2.7	ND
Removal efficiency (%)	90.4%	5.1%	4.0%	12.5%	1.3%	4.4%	5.6%	2.9%	--

252 Note: ND stands for not detected. All experiments were performed in triplicate.

253 As the Fig 4 show, through the first treatment, the recovery rate of gold was 90.4%. After the
 254 second treatment, the gold recovery dropped to 82.3%. The gold recovery rates were 61.8% and
 255 29.6% at third and fourth treatment, respectively. With four cycles, we can recover 478 mg of gold
 256 per gram of bacteria from the aqua regia-based metal wastewater.

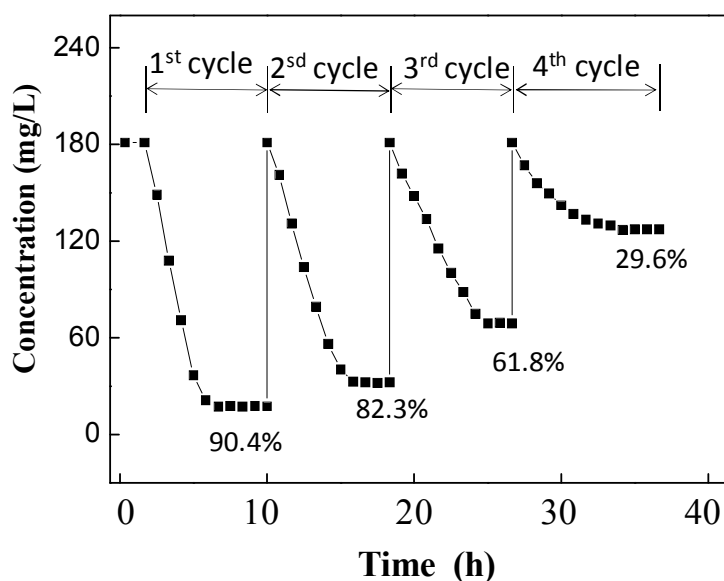


Fig 4. The *Bacillus licheniformis* FZUL-63 selectively mineralizes and recovers gold from aqua regia-based metal wastewater through four cycles.

257
258
259
260

4. Conclusion

261 An indigenous bacterium *Bacillus licheniformis* FZUL-63 was shown to selectively mineralize
262 and precipitate gold from coexisting ions in aqueous solution. The process is as follows: Au(III) ions
263 are reduced to monovalent by the *B. licheniformis*, and then the Au(I) was adsorbed on the bacterial
264 surface at the beginning stage. The amino, carboxyl and phosphate groups on the surface of the bacteria
265 are related to the adsorption of gold ions. The gold biomineralization has been rarely influenced by
266 other co-existing metal ions. The bacteria could recover 478 mg/g(dry biomass) gold from aqua regia-
267 based metal wastewater through 4 times.
268

269

Acknowledgments

270 This work was financially supported by the National Basic Research Program of China
271 (973 Program) (no. 2014CB846003), the National Natural Science Foundation of China (no.
272 41372346, 21477129) and Natural Science Foundation of Fujian Province (no. 2019J01246).
273 Additional support was provided by the China Scholarship Council (no. 201506655045).
274

275
276
277
278
279
280
281
282
283

284 **References:**

- 285 1. Yin, P.; Xu, M. Y.; Qu, R. J.; Chen, H.; Liu, X. G.; Zhang, J.; Xu, Q., Uptake of gold (III) from waste
286 gold solution onto biomass-based adsorbents organophosphonic acid functionalized spent buckwheat
287 hulls. *Bioresource technology* **2013**, *128*, 36-43, 10.1016/j.biortech.2012.10.048
- 288 2. Fan, R. Y.; Xie, F.; Guan, X. L.; Zhang, Q. L.; Luo, Z. R., Selective adsorption and recovery of Au(III)
289 from three kinds of acidic systems by persimmon residual based bio-sorbent: A method for gold
290 recycling from e-wastes. *Bioresource technology* **2014**, *163*, 167-171, 10.1016/j.biortech.2014.03.164
- 291 3. Kwak, I. S.; Yun, Y. S., Recovery of zero-valent gold from cyanide solution by a combined method
292 of biosorption and incineration. *Bioresource technology* **2010**, *101* (22), 8587-8592,
293 10.1016/j.biortech.2010.06.080
- 294 4. Hyder, M. K. M. Z.; Ochiai, B., Selective recovery of Au(III), Pd(II), and Ag(I) from printed circuit
295 boards using cellulose filter paper grafted with polymer chains bearing thiocarbamate moieties.
296 *Microsyst Technol* **2018**, *24* (1), 683-690, 10.1007/s00542-017-3277-0
- 297 5. Choudhary, B. C.; Paul, D.; Borse, A. U.; Garole, D. J., Surface functionalized biomass for
298 adsorption and recovery of gold from electronic scrap and refinery wastewater. *Sep Purif Technol* **2018**,
299 *195*, 260-270, 10.1016/j.seppur.2017.12.024
- 300 6. Van Eygen, E.; De Meester, S.; Tran, H. P.; Dewulf, J., Resource savings by urban mining: The case
301 of desktop and laptop computers in Belgium. *Resour Conserv Recy* **2016**, *107*, 53-64,
302 10.1016/j.resconrec.2015.10.032
- 303 7. Syed, S., Recovery of gold from secondary sources-A review. *Hydrometallurgy* **2012**, *115*, 30-51
- 304 8. Sheel, A.; Pant, D., Recovery of gold from electronic waste using chemical assisted microbial
305 biosorption (hybrid) technique. *Bioresource technology* **2018**, *247*, 1189-
306 1192.10.1016/j.biortech.2017.08.212
- 307 9. Alzate, A.; Lopez, M. E.; Serna, C., Recovery of gold from waste electrical and electronic
308 equipment (WEEE) using ammonium persulfate. *Waste Manage* **2016**, *57*, 113-120,
309 10.1016/j.wasman.2016.01.043
- 310 10. Natarajan, G.; Ting, Y. P., Gold biorecovery from e-waste: An improved strategy through spent
311 medium leaching with pH modification. *Chemosphere* **2015**, *136*, 232-238,
312 10.1016/j.chemosphere.2015.05.046
- 313 11. Yap, C. Y.; Mohamed, N., An electrogenerative process for the recovery of gold from cyanide
314 solutions. *Chemosphere* **2007**, *67* (8), 1502-1510, 10.1016/j.chemosphere.2006.12.017
- 315 12. Ju, X. H.; Igarashi, K.; Miyashita, S.; Mitsushashi, H.; Inagaki, K.; Fujii, S. I.; Sawada, H.; Kuwabara, T.;
316 Minoda, A., Effective and selective recovery of gold and palladium ions from metal wastewater using a
317 sulfotermophilic red alga, *Galdieria sulphuraria*. *Bioresource technology* **2016**, *211*, 759-764,
318 10.1016/j.biortech.2016.01.061
- 319 13. Kaksonen, A. H.; Mudunuru, B. M.; Hackl, R., The role of microorganisms in gold processing and
320 recovery-A review. *Hydrometallurgy* **2014**, *142*, 70-83, 10.1016/j.hydromet.2013.11.008
- 321 14. Das, N., Recovery of precious metals through biosorption - A review. *Hydrometallurgy* **2010**, *103*
322 (1-4), 180-189, 10.1016/j.hydromet.2010.03.016
- 323 15. Zhang, T.; Tu, Z. H.; Lu, G. N.; Duan, X. C.; Yi, X. Y.; Guo, C. L.; Dang, Z., Removal of heavy metals
324 from acid mine drainage using chicken eggshells in column mode. *J Environ Manage* **2017**, *188*, 1-8,
325 10.1016/j.jenvman.2016.11.076
- 326 16. Malhotra, A.; Dolma, K.; Kaur, N.; Rathore, Y. S.; Ashish; Mayilraj, S.; Choudhury, A. R.,
327 Biosynthesis of gold and silver nanoparticles using a novel marine strain of *Stenotrophomonas*.
328 *Bioresource technology* **2013**, *142*, 727-731, 10.1016/j.biortech.2013.05.109
- 329 17. Johnston, C. W.; Wyatt, M. A.; Li, X.; Ibrahim, A.; Shuster, J.; Southam, G.; Magarvey, N. A., Gold
330 biomineralization by a metallophore from a gold-associated microbe. *Nature Chemical Biology* **2013**, *9*
331 (4), 241-243, 10.1038/NChemBio.1179
- 332 18. Nita, R.; Trammell, S. A.; Ellis, G. A.; Moore, M. H.; Soto, C. M.; Leary, D. H.; Fontana, J.;
333 Talebzadeh, S. F.; Knight, D. A., Kinetic analysis of the hydrolysis of methyl parathion using citrate-
334 stabilized 10 nm gold nanoparticles. *Chemosphere* **2016**, *144*, 1916-1919,
335 10.1016/j.chemosphere.2015.10.036
- 336 19. Uebe, R.; Schuler, D., Magnetosome biogenesis in magnetotactic bacteria. *Nat Rev Microbiol*
337 **2016**, *14* (10), 621-637, 10.1038/nrmicro.2016.99
- 338 20. Amor, M.; Busigny, V.; Louvat, P.; Gelabert, A.; Cartigny, P.; Durand-Dubief, M.; Ona-Nguema, G.;
339 Alphandery, E.; Chebbi, I.; Guyot, F., Mass-dependent and -independent signature of Fe isotopes in
340 magnetotactic bacteria. *Science* **2016**, *352* (6286), 705-708, 10.1126/science.aad7632

- 341 21. Lu, A. H.; Li, Y.; Jin, S., Interactions between Semiconducting Minerals and Bacteria under Light.
342 *Elements* **2012**, *8* (2), 125-130, 10.2113/gselements.8.2.125
- 343 22. Pavlova, L. M.; Radomskaya, V. I., Biomineralization of Precious Metals. *Biogenic-Abiogenic*
344 *Interactions In Natural And Anthropogenic Systems* **2016**, 15-27.10.1007/978-3-319-24987-2_3
- 345 23. Narayanan, K. B.; Park, H. H.; Han, S. S., Synthesis and characterization of biomatrixed-gold
346 nanoparticles by the mushroom *Flammulina velutipes* and its heterogeneous catalytic potential.
347 *Chemosphere* **2015**, *141*, 169-175, 10.1016/j.chemosphere.2015.06.101
- 348 24. Reith, F.; Etschmann, B.; Grosse, C.; Moors, H.; Benotmane, M. A.; Monsieurs, P.; Grass, G.;
349 Doonan, C.; Vogt, S.; Lai, B.; Martinez-Criado, G.; George, G. N.; Nies, D. H.; Mergeay, M.; Pring, A.;
350 Southam, G.; Brugger, J., Mechanisms of gold biomineralization in the bacterium *Cupriavidus*
351 *metallidurans*. *Proceedings of the National Academy of Sciences of the United States of America* **2009**,
352 *106* (42), 17757-17762, 10.1073/pnas.0904583106
- 353 25. Das, S. K.; Liang, J.; Schmidt, M.; Laffir, F.; Marsili, E., Biomineralization Mechanism of Gold by
354 Zygomycete Fungi *Rhizopus oryzae*. *Acs Nano* **2012**, *6* (7), 6165-6173, 10.1021/nn301502s
- 355 26. Lengke, M. F.; Fleet, M. E.; Southam, G., Morphology of gold nanoparticles synthesized by
356 filamentous cyanobacteria from gold(I)-thiosulfate and gold(III)-chloride complexes. *Langmuir* **2006**,
357 *22* (6), 2780-2787, 10.1021/la052652c
- 358 27. Lin, W. T.; Huang, Z.; Li, X. Z.; Liu, M. H.; Cheng, Y. J., Bio-remediation of acephate-Pb(II)
359 compound contaminants by *Bacillus subtilis* FZUL-33. *J Environ Sci-China* **2016**, *45*, 94-99,
360 10.1016/j.jes.2015.12.010
- 361 28. Cheng, Y. J., Zhang, L., Bian, X. J. et al. , Adsorption and mineralization of REE—lanthanum onto
362 bacterial cell surface. *Environ Sci Pollut Res* **2017**, <https://doi.org/10.1007/s11356-017-9691-0>
363
- 364 29. Cheng, Y. J.; Xu, X. Y.; Yan, S. G.; Pan, X. H.; Chen, Z.; Lin, Z., Hydrothermal growth of large-size
365 UO₂ nanoparticles mediated by biomass and environmental implications. *Rsc Adv* **2014**, *4* (107),
366 62476-62482, 10.1039/c4ra10428e
- 367 30. Singh, R.; Dong, H. L.; Liu, D.; Zhao, L. D.; Marts, A. R.; Farquhar, E.; Tierney, D. L.; Almquist, C. B.;
368 Briggs, B. R., Reduction of hexavalent chromium by the thermophilic methanogen
369 *Methanothermobacter thermoautotrophicus*. *Geochim Cosmochim Acta* **2015**, *148*, 442-456,
370 10.1016/j.gca.2014.10.012
- 371 31. Bao, X. Q.; Qin, Z.; Zhou, T. S.; Deng, J. J., In-situ generation of gold nanoparticles on MnO₂
372 nanosheets for the enhanced oxidative degradation of basic dye (Methylene Blue). *J Environ Sci-China*
373 **2018**, *65*, 236-245, 10.1016/j.jes.2017.03.003
- 374 32. Miah, A.; Malakar, B.; Saikia, P., Gold over Ceria-Titania Mixed Oxides: Solar Light Induced
375 Catalytic Activity for Nitrophenol Reduction. *Catal Lett* **2016**, *146* (2), 291-303, 10.1007/s10562-015-
376 1644-y
- 377 33. Choudhary, S.; Sar, P., Uranium biomineralization by a metal resistant *Pseudomonas aeruginosa*
378 strain isolated from contaminated mine waste. *J Hazard Mater* **2011**, *186* (1), 336-343,
379 10.1016/j.jhazmat.2010.11.004
- 380 34. Pagnanelli, F.; Papini, M. P.; Toro, L.; Trifoni, M.; Veglio, F., Biosorption of metal ions on
381 *Arthrobacter* sp.: Biomass characterization and biosorption modeling. *Environ Sci Technol* **2000**, *34*
382 (13), 2773-2778, 10.1021/es991271g
- 383 35. Jiang, W.; Saxena, A.; Song, B.; Ward, B. B.; Beveridge, T. J.; Myneni, S. C. B., Elucidation of
384 functional groups on gram-positive and gram-negative bacterial surfaces using infrared spectroscopy.
385 *Langmuir* **2004**, *20* (26), 11433-11442, 10.1021/la049043+
386